Physica E 46 (2012) 97–104

Contents lists available at SciVerse ScienceDirect

Physica E

journal homepage: www.elsevier.com/locate/physe

Coupled electromechanical effects in wurtzite quantum dots with wetting layers in gate controlled electric fields: The multiband case

Sanjay Prabhakar [a,*], Roderick V.N. Melnik [a,b,c], Pekka Neittaanmäki [b], Timo Tiihonen [b]

[a] M²NeT Laboratory, Wilfrid Laurier University, Waterloo, Ontario, Canada N2L 3C5
[b] Department of Mathematical Information Technology, University of Jyväskylä, 40014, Finland
[c] Ikerbasque, Basque Foundation for Science and BCAM, 48011 Bilbao, Spain

HIGHLIGHTS

- The paper quantifies the electromechanical effects on the band structure of wurtzite quantum dots.
- Systematic study of intra-subband energies based on 2-, 6- and 8-bands k.p method has been performed.
- Non-parabolicity terms in the effective mass approximation theories have been analyzed in detail.
- The influence of the gate controlled electric fields on the intra-subband energy is explored.

ARTICLE INFO

Article history:
Received 30 December 2011
Received in revised form
29 May 2012
Accepted 24 August 2012
Available online 25 September 2012

ABSTRACT

We quantify the influence of coupled electromechanical effects on the band structure calculations of wurtzite AlN/GaN quantum dots with wetting layers (WLs). Based on a strain dependent fully coupled 8-band $\mathbf{k}\cdot\mathbf{p}$ method, we computed eigenvalues and wavefunctions of electrons in quantum dots with WLs of different aspect ratios. These computed eigenvalues are compared to those obtained from the method based on decoupled 2-conduction and 6-valence bands envelope functions. Previously, such comparisons, accounting for the wetting layer, were systematically done only for models based on not more than 4-bands. In addition, we apply gate potential along z-direction to bring the conduction and valence bands closer so that we numerically estimate the influence of gate controlled electric fields on the intra-subband energy in quantum dots. Due to the non-parabolicity term in the effective mass approximation, our study shows that the intra-sub band energy (i.e., the energy difference between ground and first excited states) is smaller for electrons and larger for holes in the 8-band $\mathbf{k}\cdot\mathbf{p}$ method than those eigenvalues obtained from the decoupled 2-conduction and 6-valence bands envelope functions method. In this paper, we show that the intra-sub band energy increases in presence of piezo-electromechanical effects and externally applied gate potentials along z-direction. We numerically estimate the distribution (i.e., the probability density) of electrons and holes wavefunctions in the dots that is obtained from both the 8-band $\mathbf{k}\cdot\mathbf{p}$ method and the decoupled 2- and 6-bands envelope functions method.

1. Introduction

Self-assembled semiconductor quantum dots (QDs) with wetting layers, grown by Stranski–Krastanov growth process, are very promising candidates to make optoelectronic devices such as light emitting diodes, lasers and components of spintronic logic devices [1–3]. The current state of the art in semiconductor technology based on the use of Molecular Beam Epitaxy (MBE), Metal Oxide Chemical Vapor Deposition (MOCVD), and other techniques allows us to precisely control the shape and size of the self-assembled quantum dots [4,5].

It is well known that mechanical phenomena such as electromechanical (EM) effects i.e., strain and piezoelectric fields have major contributions in the band structure calculations of quantum dots with WLs [6–18]. The strain is induced due to the lattice mismatch at the interfaces of AlN/GaN quantum dots [19,20]. We focus our study of the band diagram of experimentally grown GaN quantum dots with wetting layers. In this case, the height of the QDs, thickness of the WLs, temperatures during the growth process can be treated as realistic physical parameters for the design of optoelectronic devices [21,22]. The WLs have quite significant influence on the strain and piezoeletric fields, leading

* Corresponding author.
E-mail address: sprabhakar@wlu.ca (S. Prabhakar).

1386-9477/$ - see front matter © 2012 Elsevier B.V. All rights reserved.
http://dx.doi.org/10.1016/j.physe.2012.08.024

to a modification of the band diagram [7,6]. Since GaN is a highly piezoelectric material which brings the quantum states to the top of the dot for electrons and to the bottom of the dot, near the wetting layer, for holes, the influence of electromechanical effects on the quantum dots should be treated based on coupled physics considerations.

Electromechanical effects on the band structure calculations of truncated pyramidal zinc-blende and wurtzite quantum dots have been extensively studied by utilizing the envelope-function method in the effective-mass approximation and in the Kane model via both the atomistic calculations approach and the $\mathbf{k}\cdot\mathbf{p}$ method [23–26]. Our study is different in that we employ the finite element method to characterize the electronic properties of truncated pyramidal shape of wurtzite AlN/GaN quantum dots of hexagon base with wetting layers, based on the fully coupled strain dependent 8-band $\mathbf{k}\cdot\mathbf{p}$ method. We show that the intra-sub band energy increases in the presence of piezo-electromechanical effects and gate induced electric fields along z-direction.

In this paper, based on the fully coupled strain dependent 8-band $\mathbf{k}\cdot\mathbf{p}$ method, for the first time, we analyze in detail the influence of electromechanical effects on the band structure calculations of truncated pyramidal GaN quantum dots with wetting layers in the presence of externally applied electric field along z-direction. Such analysis has not been carried out before. The eigenvalues for electrons and holes, obtained from the fully coupled 8-band $\mathbf{k}\cdot\mathbf{p}$ method, are compared to the values obtained from decoupled 2-conduction and 6-valence bands envelope functions methods. Again, a systematic comparison of this type, accounting for the wetting layer, was done only for models based on not more than 4-bands (see Ref. [24,25]). We show that the conduction and valence bands can be brought closer with the application of piezo-electromechanical effects and the externally applied gate controlled electric fields along z-direction. In this case, our study shows that the intra-sub band energy of electrons and holes in quantum dots increases.

The paper is organized as follows. In Section 2, we provide details on the theoretical model for the electromechanical parts of wurtzite AlN/GaN quantum dots. Based on our theoretical model, we numerically calculate the material constants parameters in Section 3. In Section 4, we focus on the Hamiltonian for the dots based on the strain dependent 8-band $\mathbf{k}\cdot\mathbf{p}$ method in the effective mass approximation. Finally, in Section 5, for the first time in the literature, we present a detailed comparison study of the influence of piezo-electromechanical effects on the band structure of AlN/GaN quantum dots, accounting for the wetting layer. We conclude in Section 6.

2. Theoretical model for piezo-electromechanical effects

Free elastic energy of a crystal of hexagon shape can be written as [20]

$$F=\int_V dr\sum_{iklm}\frac{1}{2}C_{iklm}\varepsilon_{ik}(r)\varepsilon_{lm}(r), \tag{1}$$

where C_{iklm} are the elastic moduli constants and ε_{ik} are the components of strain tensors. The strain tensor components can be obtained by minimizing the free elastic energy over the total volume V. This can be generalized to the electroelastic energy and, as the result, the coupled system of the Navier equations for stress and Maxwel's equations for piezoelectric fields can be written as [27]

$$\partial_j\sigma_{ik}=0, \tag{2}$$

$$\partial_i D_i=0. \tag{3}$$

The stress tensor components σ_{ik} and the electric displacement vector components D_i can be written as

$$\sigma_{ik}=C_{iklm}\varepsilon_{lm}+e_{nik}\partial_n V, \tag{4}$$

$$D_i=e_{ilm}\varepsilon_{lm}-\hat{\epsilon}_{in}\partial_n V+P_{sp}\delta_{iz}, \tag{5}$$

where e_{ik} is the piezoelectric constant, ϵ_{in} is the permittivity, V is the piezoelectric potential, P_{sp} is the spontaneous polarization and $E=-\frac{\partial V}{\partial z}$ is the built in piezoelectric field. Further details of the analysis of Eqs. (2)–(5) can be found in Refs. ([28,27,29–31]). Here we only notice that the coupled formulation of Eqs. (2)–(5) is essential and the minimization of pure elastic energy of Eq. (1), rather than the full electroelastic energy, may lead to substantial errors, when applied to modeling of low dimensional nanostructures (see Ref. [6] and references therein). It is also well known that the internal strain may lead to a reduced band gap in such structures, influencing the quantum confinement effect [32]. In what follows, we apply the Lifshits–Rosentsverg theory that accounts for such a strain [33,34]. In this case, the standard Cauchy strain and the internal strain due to lattice mismatch have the form:

$$\varepsilon_{ij}=\varepsilon^u_{ij}+\varepsilon^0_{ij}, \tag{6}$$

where ε^0_{ij} are the local intrinsic strain tensor components due to lattice mismatch and ε^u_{ij} is position dependent strain tensor components. These two can be written as

$$\varepsilon^0_{ij}=(\delta_{ij}-\delta_{iz}\delta_{jz})a+\delta_{iz}\delta_{jz}c, \tag{7}$$

$$\varepsilon^u_{ij}=\tfrac{1}{2}(\partial_j u_i+\partial_i u_j), \tag{8}$$

where $a=(a_0-a)/a_0$ and $c=(c_0-c)/c_0$ in the dot and zero in the matrix. Here, a_0, c_0 and a, c are the lattice constants of the dot and the matrix along a and c directions respectively.

3. Material parameters

The piezoelectric tensors e_{ik} can be written in the form of the tensors of d_{il} and the tensors of $C_{iklm}=C_{il}$ as [35,36]

$$e_{ij}=\sum_{k=1}^{6}d_{ik}C_{il}, \tag{9}$$

which can be transformed into the following expressions for wurtzite:

$$e_{31}=d_{31}C_{11}+d_{33}C_{13}, \tag{10}$$

$$e_{33}=d_{31}C_{13}+d_{33}C_{33}, \tag{11}$$

$$e_{15}=d_{15}C_{55}=d_{15}C_{44}. \tag{12}$$

Thus obtained components of the tensor $\mathbf{e}$ are summarized in Table 1 for GaN and AlN.

4. Hamiltonian of Kane model for wurtzite quantum dots

The interaction of electrons in the conduction bands and holes in the valence bands can be explained by the Kane Hamiltonian. However, the effects of the remote bands on these conduction and valence bands can be calculated by second order perturbation theory [39,19,40–42]. The steady state Schrödinger equation of the Kane model can be written as

$$\mathbf{H}\boldsymbol{\psi}=E\boldsymbol{\psi}, \tag{13}$$

where

$$\mathbf{H}=\begin{pmatrix}\mathbf{H_c} & \mathbf{H_{cv}}\\ \mathbf{H^{\dagger}_{cv}} & \mathbf{H_v}\end{pmatrix},\quad \boldsymbol{\psi}=\begin{pmatrix}\boldsymbol{\psi_c}\\ \boldsymbol{\psi_v}\end{pmatrix}, \tag{14}$$

Table 1
Lattice parameters of wurtzite GaN and AlN used in computation. If not indicated differently, they are taken from Ref. [37].

Parameter	GaN	AlN
a_0 (Å)	3.189	3.112
c_0 (Å)	5.185	4.982
c_{11} (GPa)	390	396
c_{12} (GPa)	145	137
c_{13} (GPa)	106	108
c_{33} (GPa)	398	373
c_{44} (GPa)	105	116
d_{31} (pm/V)	−1.6	−2.1
d_{33} (pm/V)	3.1	5.4
d_{15} (pm/V)	3.1	3.6
P_{sp} (C/m^2)	−0.034	−0.090
e_{31} (C/m^2)	−0.30[a]	−0.25[a]
e_{33} (C/m^2)	1.06[a]	1.79[a]
e_{15} (C/m^2)	0.33[a]	0.42[a]
κ_1	10.06[b]	8.57[b]
κ_2	9.28[b]	8.67[b]

[a] Derived from expressions (10).
[b] Ref. [38].

with $\boldsymbol{\psi_c}=\boldsymbol{\psi_c}(\mathbf{r})$ being the position dependent conduction band envelope function and $\boldsymbol{\psi_v}=\boldsymbol{\psi_v}(\mathbf{r})$ being the position dependent valence band envelope function. The total wave function $\boldsymbol{\Psi}$ is [43]

$$\boldsymbol{\Psi}=\sum_{j=c,x,y,z}\phi_j\psi_j=\boldsymbol{\phi}\boldsymbol{\psi}, \tag{15}$$

where, $\boldsymbol{\phi}=(\phi_c\phi_x\phi_y\phi_z)$ and $\boldsymbol{\psi}=(\psi_c\psi_x\psi_y\psi_z)^T$. The functions $\boldsymbol{\phi}$ are spinless and $\boldsymbol{\psi}$ is a spinor

$$\boldsymbol{\psi}_j=\begin{pmatrix}\psi_j^1\\ \psi_j^2\end{pmatrix},\quad j=c,x,y,z. \tag{16}$$

Hence, the basis functions of the Hamiltonian (14) have the following form [43]:

$$(\phi_c\psi_c^1\ \ \phi_x\psi_x^1\ \ \phi_y\psi_y^1\ \ \phi_z\psi_z^1\ \ \phi_c\psi_c^2\ \ \phi_x\psi_x^2\ \ \phi_z\psi_z^2\ \ \phi_z\psi_z^2)^T.$$

We now turn to the description of the matrix Hamiltonian $\mathbf{H}$ of (14). The diagonal element of the intra-conduction band Hamiltonian $\mathbf{H_c}$ can be written as

$$H_c=A_1'k_z^2+A_2'(k_x^2+k_y^2)+U_c +ef_zz+a_1\varepsilon_{zz}+a_2(\varepsilon_{xx}+\varepsilon_{yy}), \tag{17}$$

where $U_c=U_c(\mathbf{r})$ is the position dependent edge of the conduction band Γ_1, which also includes an external scalar potential present, a_1 and a_2 are deformation potentials for the conduction band and, as before, ε_{ij} are the components of strain tensor. Here, f_z is the externally applied electric field along the z-direction. The parameters A_1' and A_2' are expressed via the components $1/m_\parallel$ and $1/m_\perp$ of the tensor of the reciprocal effective masses for the conduction band in the single-band approximation and the Kane parameters $P_1=-i\hbar\langle\phi_c|\hbar k_z|\phi_z\rangle/m_0$ and $P_2=-i\hbar\langle\phi_c|\hbar k_x|\phi_x\rangle/m_0$. They are given by

$$A_1'=\frac{\hbar^2}{2m_\parallel}-\frac{P_1^2}{E_g}, \tag{18}$$

$$A_2'=\frac{\hbar^2}{2m_\perp}-\frac{P_2^2}{E_g}, \tag{19}$$

where E_g is the band gap of wurtzite semiconductor materials.

The intra-valence-band Hamiltonian $\mathbf{H}_v$ can be written as

$$\mathbf{H_v}=\mathbf{H^{(0)}}+\mathbf{H^{(so)}}+\mathbf{H}^{(\varepsilon)}+\mathbf{H}'^{(\mathbf{k})}. \tag{20}$$

The Hamiltonian $\mathbf{H^{(0)}}$ entering Eq. (20) represents the position-dependent potential energy of an electron

$$\mathbf{H^{(0)}}=\begin{pmatrix}U_{v6}&0&0\\0&U_{v6}&0\\0&0&U_{v1}\end{pmatrix}+ef_zz, \tag{21}$$

where $U_{v6}=U_{v6}(\mathbf{r})$ and $U_{v1}=U_{v1}(\mathbf{r})$ are the position dependent edges of the valence bands Γ_6 and Γ_1 respectively, which also include an externally applied electric field, f_z, along z-direction.

The spin-orbit Hamiltonian $\mathbf{H^{(so)}}$ in Eq. (20) can be treated as a perturbation term. Based on first order perturbation theory, the spin-orbit Hamiltonian $\mathbf{H^{(so)}}$ can be expressed in terms of Pauli spin matrices [44] by neglecting small linear terms in the momentum operator [19]. $\mathbf{H_{so}}$ can be written as

$$\mathbf{H^{(so)}}=i\begin{pmatrix}0&-\Delta_2\sigma_z&\Delta_3\sigma_y\\ \Delta_2\sigma_z&0&-\Delta_3\sigma_x\\ -\Delta_3\sigma_y&\Delta_3\sigma_x&0\end{pmatrix}, \tag{22}$$

where $\Delta_2=\Delta_2(\mathbf{r})$ and $\Delta_3=\Delta_3(\mathbf{r})$ are parameters of the valence-band spin-orbit splitting [44], and σ_x, σ_y and σ_z are the Pauli matrices

$$\sigma_x=\begin{pmatrix}0&1\\1&0\end{pmatrix},\quad \sigma_y=\begin{pmatrix}0&-i\\i&0\end{pmatrix},\quad \sigma_z=\begin{pmatrix}1&0\\0&-1\end{pmatrix}. \tag{23}$$

The kinetic energy Hamiltonian $\mathbf{H}'^{(\mathbf{k})}$ in Eq. (20) can be written as [43]

$$\mathbf{H}'^{(\mathbf{k})}=\begin{pmatrix}L_1'k_x^2+M_1k_y^2+M_2k_z^2 & N_1'k_xk_y & N_2'k_xk_z\\ N_1'k_xk_y & M_1k_x^2+L_1'k_y^2+M_2k_z^2 & N_2'k_yk_z\\ N_2'k_xk_z & N_2'k_yk_z & M_3\left(k_x^2+k_y^2\right)+L_2'k_z^2\end{pmatrix}, \tag{24}$$

where

$$L_1'=L_1+\frac{P_1^2}{E_g},\quad L_2'=L_2+\frac{P_2^2}{E_g}, \tag{25}$$

$$N_1'=N_1+\frac{P_1^2}{E_g},\quad N_2'=N_2+\frac{P_1P_2}{E_g}. \tag{26}$$

For the interband block $\mathbf{H_{cv}}$ of the Hamiltonian (14) ($\mathbf{H_{cv}^\dagger}$ is its Hermitian conjugate) we have

$$\mathbf{H_{cv}}=(H_{cx}\ \ H_{cy}\ \ H_{cz}), \tag{27}$$

where

$$H_{cx}=iP_2k_x,\quad H_{cy}=iP_2k_y,\quad H_{cz}=\ iP_1k_z. \tag{28}$$

5. Results and discussions

We consider hexagonal GaN quantum dots of truncated pyramidal shape with wetting layers. The quantum dots are embedded in the matrix of AlN materials of hexagon base symmetry. The schematic diagram of the geometry is shown in Fig. 1. We consider $b=15$ nm as a lateral size of the dot. The height of the dot (h) varies from 3 nm to 5 nm with 1 nm thick wetting layer. These parameters of the dot mimic the realistic shapes and sizes of the physical structures that were reported experimentally in Refs. [21] and [22]. The constants for AlN and GaN materials are listed in Table 2.

In Fig. 2, we demonstrate the influence of piezo-electromechanical effects on the flat bands and on the bands of gate controlled electric fields $f_z=10^6$ V/cm of the dot along z-direction. In this figure, solid lines (black) represent the flat bands and the dotted lines (red) represent the influence of piezo-electromechanical effects on the flat bands of the dots. Also, dashed lines (magenta) represent the effect of gate induced electric fields, $f_z=10^6$ V/cm on the flat bands and dashed-dotted lines

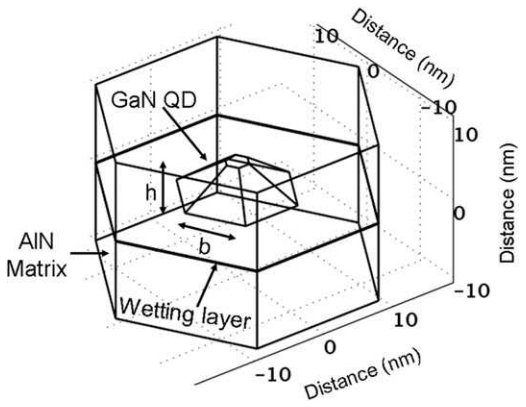

Fig. 1. Schematic diagram of a AlN/GaN quantum dot with the actual shape of hexagonal truncated pyramid, mounted on a thin wetting layer. Here the adjustable parameter, h, is the height of the dot and b is the side length of the hexagon which is fixed in our computational work.

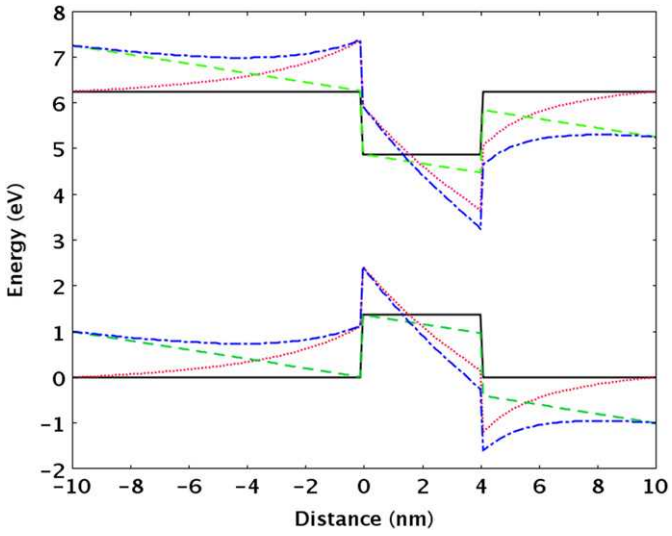

Fig. 2. Influence of piezo-electromechanical effects on the band diagram of AlN/GaN quantum dots. Solid lines (black) represent the flat band diagram and dotted lines (red) represent the piezo-electromechanical effects on the flat band diagram. Also, dashed lines (green) represent the band diagram of gate induced electric fields at $f_z = 10^6$ V/cm and dashed-dotted lines represent (blue) the piezo-electromechanical effects on the band diagram of gate induced electric fields at $f_z = 10^6$ V/cm. (For interpretation of the references to color in this figure caption, the reader is referred to the web version of this article.)

(blue) represent the piezo-electromechanical effects on the bands of gate induced electric fields at $f_z = 10^6$ V/cm. Due to significant piezo-electromechanical effects in wurtzite AlN/GaN quantum dots, it can be seen that the minima of the conduction bands are near the top of the dots, while maxima of the valence bands are close to the bottom of the dots, near the wetting layers. In the presence of externally applied electric field along z-direction, we see that the minima of the conduction band goes further down. For that case, we show that the effect of remote bands on the intra-sub bands energy states computed from the 8-band $\mathbf{k}\cdot\mathbf{p}$ method is significantly more profound than the effect obtained from the decoupled 2-conduction and 6-valence bands envelope functions method. This situation is interpreted by Fig. 9.

In Figs. 3 and 4, based on the strain dependent 8-band $\mathbf{k}\cdot\mathbf{p}$ method, we computed the eigenvalues and plotted ground, first and second excited states wavefunctions of electrons and holes in the bands that are considered in Fig. 2. The upper panel from left to right in Fig. 3 shows the wavefunctions of electrons in the flat conduction bands. Here, the eigenvalues of three constitutive

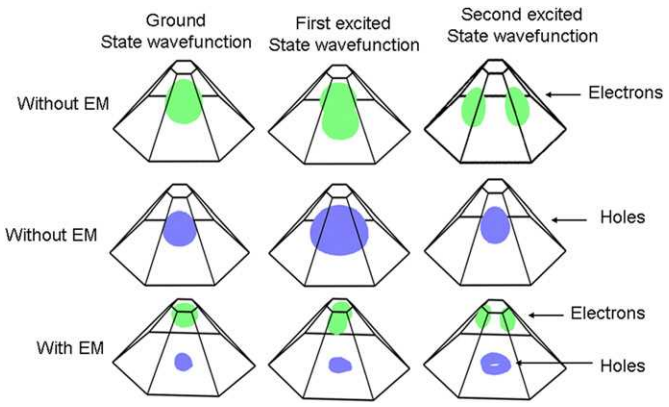

Fig. 3. The influence of piezo-electromechanical effects on the wavefunctions of electrons and holes of AlN/GaN quantum dots. (For interpretation of the references to color in this figure caption, the reader is referred to the web version of this article.)

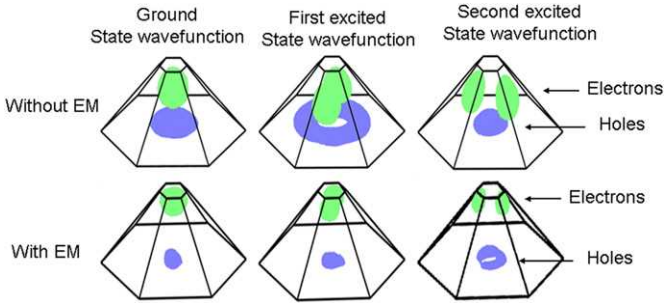

Fig. 4. The influence of piezo-electromechanical effects on the wavefunctions of electrons and holes on the bands of gate controlled electric fields at $f_z = 10^6$ V/cm for AlN/GaN quantum dots. In the upper panel, we estimate the eigenvalues as E_0=4.817677 eV, E_1=4.928222 eV and E_2=4.928253 eV for electrons in the conduction band. In the middle panel, we estimate the eigenvalues as E_0=1.273063 eV, E_1=1.271259 eV and E_1=1.264977 eV for holes in the valence band. In the lower panel, we estimate the eigenvalues as E_0=4.425142 eV, E_1=4.611962 eV and E_2=4.612804 eV for electrons in the conduction band and E_0=1.96861 eV, E_1=1.957035 eV and E_2=1.945744 eV for holes in the valence band. (For interpretation of the references to color in this figure caption, the reader is referred to the web version of this article.)

states of electrons are E_0=5.014496 eV, $E_1 = 5.091396$ eV and $E_2 = 5.091424$ eV. Middle panel from left to right in Fig. 3 shows the wavefunctions of holes in the flat valence bands. Here, the eigenvalues of three constitutive states of holes are $E_0 =$ 1.364575 eV, $E_1 = 1.362555$ eV and $E_1 = 1.357227$ eV. It can be seen that the localization of electrons and holes is in the middle of the dot, indicating that piezo-electromechanical effects are not taken into account in the 8-band $\mathbf{k}\cdot\mathbf{p}$ method. Next, we consider the influence of piezo-electromechanical effects on the eigenvalues and wavefunctions of electrons and holes in the conduction and valence bands respectively. Lower panel from left to right in Fig. 3 shows the wavefunctions of electrons and holes in the bands (dotted-red) in Fig. 2. It can be seen that the minima of piezoelectric potential for electrons are located at the top of the dot which brings the electron wavefunctions near the top of the dot. However, for the holes, maxima of piezoelectric potential are located at the bottom of the dot, near the wetting layer, which again brings the hole wavefunctions to the bottom of the dot near the wetting layer. For electrons, we estimate $E_0 = 4.74829$ eV, $E_1 = 4.920831$ eV and $E_2 = 4.921646$ eV. For holes, we estimate $E_0 = 1.988498$ eV, $E_1 = 1.97699$ eV and $E_1 = 1.965576$ eV. In Fig. 4, we see the influence of piezo-electromechanical effects on the bands of gate controlled electric fields, $f_z = 10^6$ V/cm. We plotted the electron and hole wavefunctions in the bands of dashed line (magenta) and

dashed-dotted line (blue) of Fig. 2. In Fig. 4, we also estimate the eigenvalues of electrons and holes in the conduction and valence bands (which are shown in the figure).

Table 2
Electron band structure parameters of wurtzite GaN and AlN used in computation. If not indicated differently, they are taken from Ref. [41].

Parameter	GaN	AlN
E_g (eV)	3.51	6.25
Δ_{cr} (eV)	0.034	−0.295
Δ_{so} (eV)	0.017[a]	0.019[a]
$m_{\parallel}$	$0.19m_0$	
$m_{\perp}$	$0.21m_0$	
A_1	−5.947	
A_2	−0.528	
A_3	5.414	
A_4	−2.512	
A_5	−2.510	
A_6	−3.202	
A_7 (eVÅ)	0.046	
P_1 (eVÅ)	8.1	
P_2 (eVÅ)	7.9	
a_1 (eV)	−4.9[a]	−3.4[a]
a_2 (eV)	−11.3[a]	−11.8[a]
D_1 (eV)	−3.7[a]	−17.1[a]
D_2 (eV)	4.5[a]	7.9[a]
D_3 (eV)	8.2[a]	8.8[a]
D_4 (eV)	−4.1[a]	−3.9[a]
D_5 (eV)	−4.0[a]	−3.4[a]
D_6 (eV)	−5.5[a]	−3.4[a]

[a] Ref. [37].

From Figs. 5–9, we observe the influence of piezo-electromechanical effects on the band structure calculations of wurtzite AlN/GaN quantum dots with wetting layer. Note that, in Figs. 5–9, the solid lines (black) and dashed lines (red) represent the eigenvalues obtained from the 8-band $\mathbf{k}\cdot\mathbf{p}$ method while the dotted lines (magenta) and dashed-dotted lines (blue) represent the eigenvalues obtained from decoupled 2-conduction and 6-valence bands envelope functions method. Here, we compare the eigenvalues of electrons in the conduction bands and holes in the valence bands with the variation of height, h, of the dot, keeping the lateral size constant. Due to a non-parabolicity term in the effective mass approximation, considering the flat valence band of AlN as a reference point to be zero, it can be seen that the eigenvalues of electrons in the conduction bands, obtained from the 8-band $\mathbf{k}\cdot\mathbf{p}$ are always smaller than those eigenvalues obtained from the 2-conduction bands envelope functions method. However, for holes, the eigenvalues in the valence bands, obtained from the 8-band $\mathbf{k}\cdot\mathbf{p}$ method, are higher than those eigenvalues obtained from the 6-valence bands envelope functions method from the reference point. Indeed, due to the non-parabolicity term in the effective mass approximation, the electrons have $+ve$ effective mass in the conduction bands and holes have $-ve$ effective mass in the valence bands. Below, we quantify the influence of non-parabolicity term in the effective mass approximation by utilizing the fully-coupled strain dependent 8-band $\mathbf{k}\cdot\mathbf{p}$ method.

In Fig. 5, we plotted eigenvalues of electrons in the conduction bands and holes in the valence bands with the variation of height of the dots. Since AlN/GaN quantum dots are wide band gap

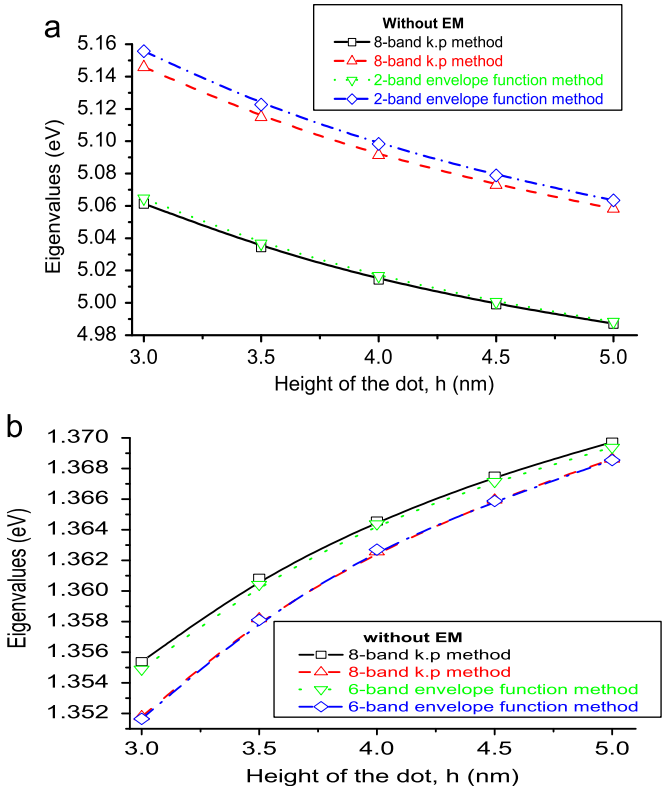

Fig. 5. Systematic study of the eigenvalues of electrons and holes with the variation of the height of the dot in bands shown by solid lines (black) in Fig. 2. Solid lines (black) and dotted lines (magenta) represent the ground state eigenvalues, while dashed lines (red) and dashed-dotted lines (blue) represent the first excited states eigenvalues for both electrons and holes in the dot. (a) Electrons and (b) Holes. (For interpretation of the references to color in this figure caption, the reader is referred to the web version of this article.)

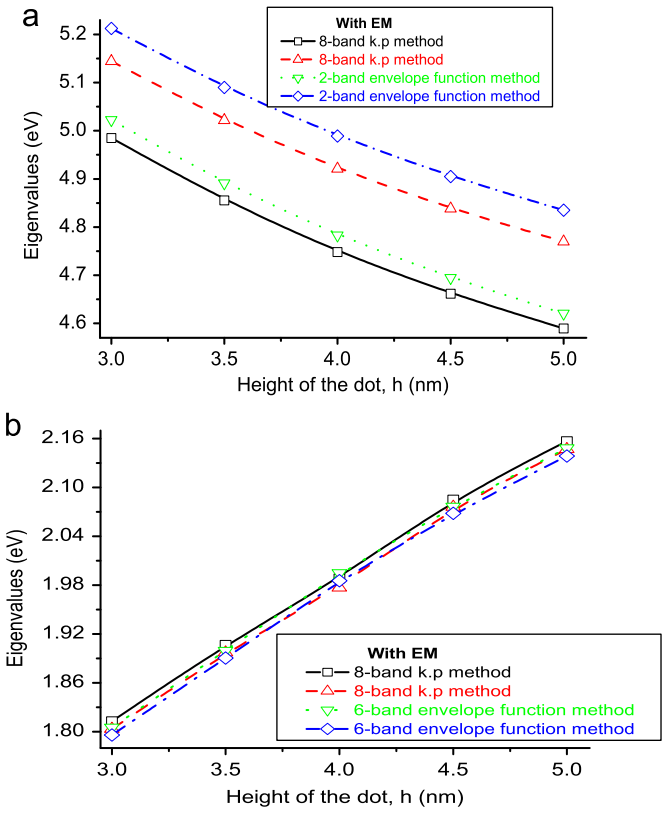

Fig. 6. Influence of piezo-electromechanical effects on the eigenvalues of electrons and holes with the variation of the height of the dot in the bands shown by dotted lines (red) in Fig. 2. Solid lines (black) and dotted lines (magenta) represent the ground state eigenvalues while dashed lines (red) and dashed-dotted lines (blue) represent the first excited states eigenvalues for both electrons and holes in the dot. (a) Electrons and (b) Holes. (For interpretation of the references to color in this figure caption, the reader is referred to the web version of this article.)

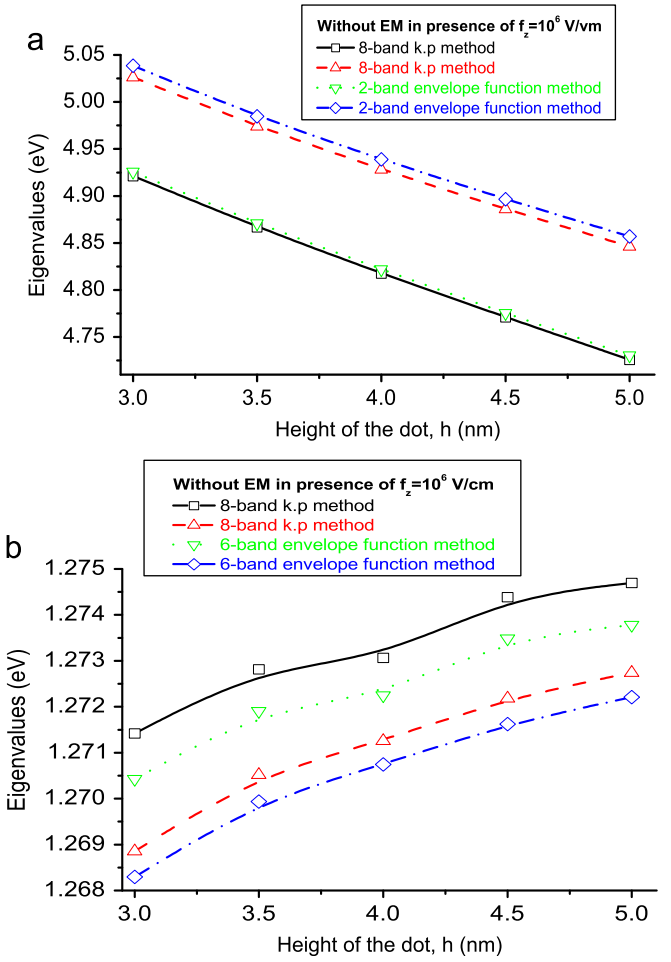

Fig. 7. Systematic study of the eigenvalues of electrons and holes with the variation of the height of the dot in the bands for the case of gate induced electric fields at $f_z = 10^6$ V/cm shown by dashed line (green) in Fig. 2. Solid lines (black) and dotted lines (magenta) represent the ground state eigenvalues while dashed lines (red) and dashed-dotted lines (blue) represent the first excited states eigenvalues for both electrons and holes in the dot. (a) Electrons and (b) Holes. (For interpretation of the references to color in this figure caption, the reader is referred to the web version of this article.)

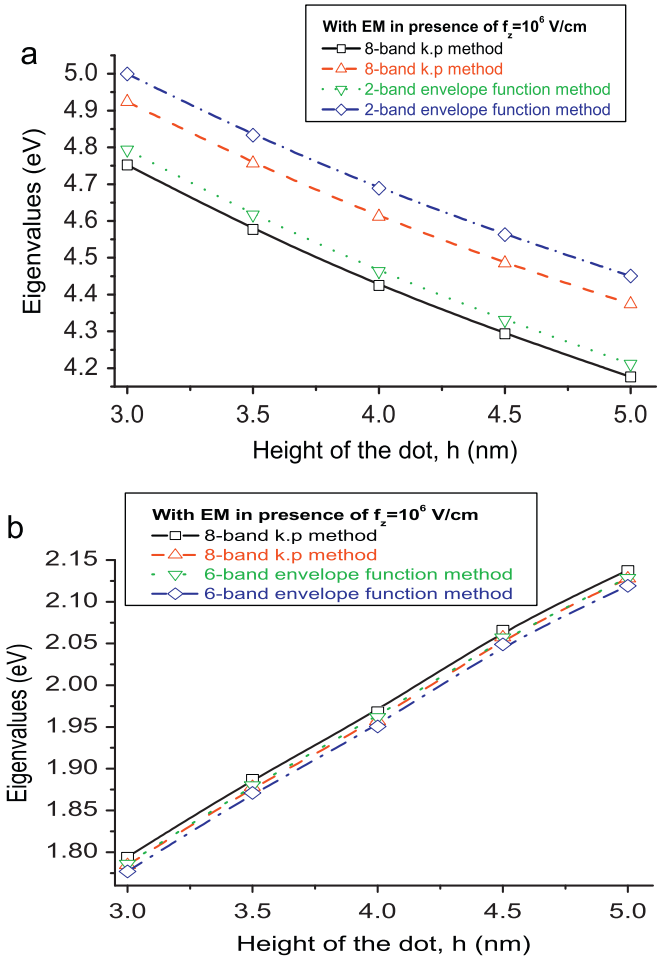

Fig. 8. Influence of piezo-electromechanical effects on the eigenvalues of electrons and holes with the variation of the height of the dot in the bands shown by dashed-dotted lines (blue) in Fig. 2. Solid lines (black) and dotted lines (green) represent the ground state eigenvalues while dashed lines (red) and dashed-dotted lines (blue) represent the first excited states eigenvalues for both electrons and holes in the dot. (a) Electrons and (b) Holes. (For interpretation of the references to color in this figure caption, the reader is referred to the web version of this article.)

semiconductor materials, the effects from the remote bands on the conduction and valence bands are very small and one can adopt the method based on decoupled 2-conduction and 6-valence bands envelope functions for the band structure calculation of wurtzite AlN/GaN quantum dots. However, the effects from the remote bands can be well pronounced if we consider the piezoelectric behavior of wurtzite AlN/GaN materials. The piezo-electromechanical effect on the band structure calculations of AlN/GaN quantum dot is shown in Fig. 6. As discussed earlier, piezo-electromechanical effect brings the minima of the conduction band further down, while the maxima of the valence bands are pushed further up by keeping the flat valence band of AlN as a reference point to be zero.

One of the key results of this paper is shown in Figs. 7 and 8. We apply the external gate induced electric field $f_z = 10^6$ V/cm along z-direction to modify the flat bands. The bands of electrons and holes in this case are shown in Fig. 2. Due to modification in the bands in the presence of electric fields along z-direction, it can be seen in Figs. 7 and 8 that we can precisely bring the eigenvalues further down for electrons in the conduction bands and further up for holes in the valence bands. In this case, the minima of the conduction bands and maxima of the valence bands come closer and the effects of the remote bands on the eigenvalues significantly increase. It means that the gate controlled electric fields along z-direction enhances the intra-sub band energy in AlN/GaN QDs with WLs.

Now, we summarize the above results in Fig. 9. We plotted intra-sub band energy of electrons versus the height of the dots. The intra-sub band energy, obtained from the 8-band $\mathbf{k}\cdot\mathbf{p}$ method (solid lines (black) and dashed lines (red)), is compared to those values, obtained from 2-conduction bands envelope functions methods (dotted line (magenta) and dashed-dotted line (blue)). In Fig. 9(a), our study shows that the eigenenergy difference, obtained from the 8-band $\mathbf{k}\cdot\mathbf{p}$ method in the flat conduction bands, is very close to the value, obtained from the 2-bands envelope functions method. In fact, the eigenenergy difference obtained from these two approaches (the 8-band $\mathbf{k}\cdot\mathbf{p}$ method and 2-bands envelope functions methods) is approximately 6 meV. However, the energy difference increases to 30 meV if we consider the piezo-electromechanical effects on the flat band of AlN/GaN quantum dots (see dashed and dashed-dotted lines in Fig. 9(a)). In the presence of gate induced electric fields along z-direction (solid and dotted lines in Fig. 9(b)), the minima of the conduction bands and maxima of the valence bands come closer. In that case, the effects of the remote bands on the eigenstates increase. We estimate the energy difference obtained from two different approaches (the 8-band $\mathbf{k}\cdot\mathbf{p}$ method

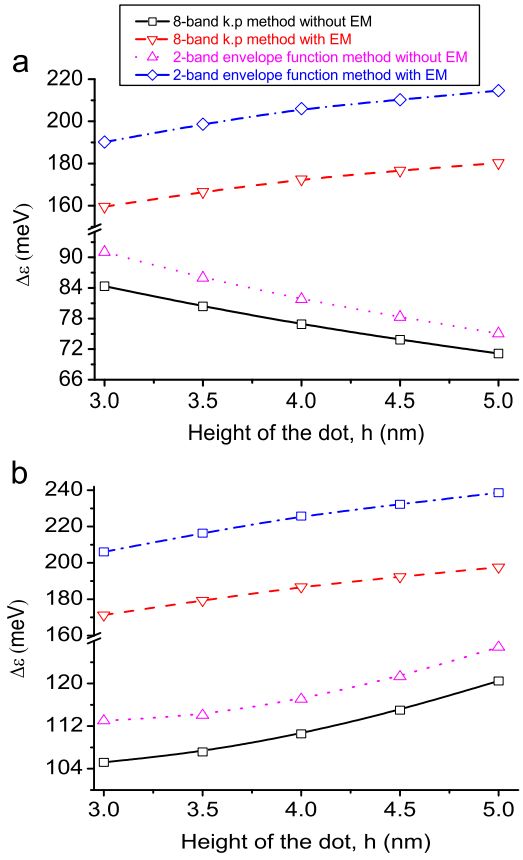

Fig. 9. Influence of piezo-electromechanical effects on intra-sub band energy i.e., the energy difference, $\triangle\varepsilon$ between ground to first excited states versus the variation of the height of the dot in the conduction bands shown in Fig. 2. In Fig. 9(a), we did not apply gate induced electric fields while in Fig. 9(b), we apply gate induced electric fields $f_z = 10^6$ V/cm. (For interpretation of the references to color in this figure caption, the reader is referred to the web version of this article.)

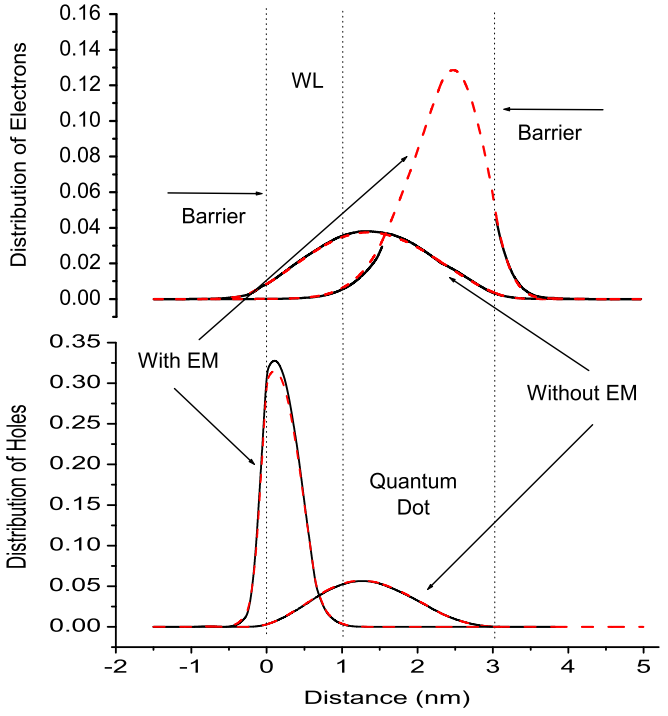

Fig. 10. Distribution (i.e., the probability density) of electrons and holes wavefunctions in AlN/GaN quantum dots versus distance along z-direction. In this plot, we estimate the probability of electrons and holes present in the AlN barrier materials and explain why the 8-band Kane model is important in the presence of piezo-electromechanical (EM) effects (see further discussions in the text). (For interpretation of the references to color in this figure caption, the reader is referred to the web version of this article.)

and 2-bands envelope functions method) as being approximately 6 meV. Keep in mind that this energy difference is approximately in the same range for the case of electrons in the flat conduction bands of the dots because the energy difference between the minima and maxima points in the bands is still large enough and the effects of the remote bands are still negligible. However, in the case of piezo-electromechanical effects on the bands of gate induced electric fields along z-direction, the energy difference between these two points (minima and maxima) is small. It means that the effects of the remote bands can be significantly pronounced. Here, we estimate that the energy difference is approximately 37 meV which is shown by upper panel in Fig. 9 (b).

In Fig. 10, we estimate the distribution (i.e., the probability density) of electrons and holes wavefunctions in AlN/GaN quantum dots, obtained from the decoupled 2- and 6-bands envelope functions method and 8-band Kane model. Solid lines (black) represent the probability density of electrons, obtained from the 8-band $\mathbf{k}\cdot\mathbf{p}$ method and dashed lines (red) represent the results obtained with the decoupled 2 and 6-band envelope functions method. We consider the height of the dots as 3 nm and estimate the piezo-electromechanical effects on the probability density of electrons and holes wavefunctions of AlN/GaN quantum dot with 1 nm thick wetting layers. In the absence of piezo-electromechanical effects, our study shows that only 6% of electrons and 0.4% of holes are distributed in the barrier materials. However, in the presence of piezo-electromechanical effects, probability density of electrons and holes in the barrier materials increases. We found that 12% of electrons and 8% of holes in this case are present in the AlN materials. In the presence of both piezo-electromechanical effects and gate controlled electric fields along z-direction, the probability density of electrons and holes in the barrier materials increases. Below, we analytically estimate the intra-sub band energy levels and compare them to the exact values, obtained from the 2, 6 and 8-bands envelope functions methods.

The analytical expression to estimate the intra-sub band energy of the dots can be written as

$$\triangle E^{estimate} = \frac{\int_b |\Psi|^2 d^3r}{\int_V |\Psi|^2 d^3r}\left(\frac{\delta E_g}{E_g}\right)|\triangle E|^{c\times c}, \tag{29}$$

$$\triangle E^{exact} = |\triangle E|^{c\times c} - |\triangle E|^{8\times 8}, \tag{30}$$

where Ψ is the wavefunction, b is the integration over the AlN barrier and V is the volume. $\triangle E$ is the intra-sub band energy, $c\times c$ denotes 2×2 conduction bands or 6×6 valence bands. E_g is the band gap of GaN and $\delta E_g = \triangle E_c + \triangle E_v$. Here, $\triangle E_c$ and $\triangle E_v$ are the band offsets in the conduction and valence bands of AlN/GaN heterojunction respectively. We suppose $\delta E_g/E_g \approx 1$ in our study. Below, we calculate $\triangle E^{estimate}$ and compare it to $\triangle E^{exact}$ for electrons and holes.

Without piezo-electromechanical effects:

For electrons:

$$\triangle E^{estimate} \approx 0.06|\triangle E|^{2\times 2} \approx 6 \text{ meV},$$

$$\triangle E^{exact} = |\triangle E|^{2\times 2} - |\triangle E|^{8\times 8} \approx 15 \text{ meV}.$$

For holes:

$$\triangle E^{estimate} \approx 0.004|\triangle E|^{6\times 6} \approx 0.01 \text{ meV},$$

$\triangle E^{exact} \approx 0.4$ meV.

With piezo-electromechanical effects:
For electrons:

$\triangle E^{estimate} \approx 0.12(190 \text{ meV}) \approx 22$ meV,

$\triangle E^{exact} \approx 31$ meV.

For holes:

$\triangle E^{estimate} \approx 0.08(9 \text{ meV}) \approx 0.7$ meV,

$\triangle E^{exact} \approx 0.4$ meV.

The above intra-sub band energy estimates, $\triangle E^{estimate}$, are in an agrement with the exact value $\triangle E^{exact}$. However, in the absence of piezo-electromechanical effects, the estimation of intra-sub-band energy for holes is one order of magnitude less than the exact value. This is because the effective masses of holes are large and the penetration of holes wave functions in the barrier is very small. As a result, it gives very close energy levels between the inter sub-band states. The error in the $\triangle E^{estimate}$ increases with the increase of the height of the dot.

6. Conclusions

In Figs. 2–4, by using the fully coupled strain dependent 8-band $\mathbf{k}\cdot\mathbf{p}$ method, we have analyzed the influence of piezo-electromechanical effects and gate controlled electric field along z-direction on the band structure calculations of wurtzite AlN/GaN quantum dots with WLs. Here we have shown that the piezo-electromechanical effect brings the localization of electron wavefunctions to the top of the dots and the localization of hole wavefunctions to the bottom of the dots near the WLs. In Figs. 5–8, we have compared the intra-sub band energy of electrons and holes. We demonstrated that, due to non-parabolicity term in the effective mass approximations methods, the eigenvalues for electrons obtained from the fully coupled 8-band $\mathbf{k}\cdot\mathbf{p}$ method are always smaller than those value obtained from the method based on 2-conduction bands envelope functions and vice-versa for holes obtained from the method based on 6-band envelope functions. Such a comparison for the quantum dots with WLs was done for the first time for fully coupled 8-band models. We have also shown that in the presence of externally applied electric fields along z-direction with piezo-electromechanical effects, the intra-sub band energy for electrons and holes increases. Finally, Fig. 10 demonstrates that the distributions of electrons and holes in the barrier materials are approximately one order of magnitude smaller in the flat band case than those values that were obtained with taking the piezo-electromechanical effects into account.

The work was carried out in M^{2}NeT Laboratory at Wilfrid Laurier University and supported by the Natural Sciences and Engineering Research Council (NSERC) and Canada Research Chair (CRC) Program, Canada. The authors thank Dr. Eduard Takhtamirov for many helpful discussions.

References

[1] L. Jacak, P. Hawrylak, A. Wójs, Semiconductor Quantum Dots, Springer, Berlin, 1998.
[2] P. Harrison, Quantum Wells, Wires and Dots, John Wiley & Sons, Ltd, 2006.
[3] J.A. Brum, P. Hawrylak, Superlattices and Microstructures 22 (1997) 431.
[4] X. Peng, L. Manna, W. Yang, J. Wickham, E. Scher, A. Kadavanich, A.P. Alivisatos, Nature 404 (2000) 59.
[5] S. Tanaka, S. Iwai, Y. Aoyagi, Applied Physics Letters 69 (1996) 4096.
[6] S. Prabhakar, R. Melnik, Journal of Applied Physics 108 (2010) 064330.
[7] S.R. Patil, R.V.N. Melnik, Nanotechnology 20 (2009) 125402.
[8] R.V.N. Melnik, M. Willatzen, Nanotechnology 15 (2004) 1.
[9] R.V.N. Melnik, K.N. Zotsenko, Modelling and Simulation in Materials Science and Engineering 12 (2004) 465.
[10] S. Park, W. Hong, Chinese Physics Letters 27 (2010) 098502.
[11] T. Nakaoka, T. Saito, J. Tatebayashi, S. Hirose, T. Usuki, N. Yokoyama, Y. Arakawa, Physics Review B 71 (2005) 205301.
[12] T. Saito, H. Ebe, Y. Arakawa, T. Kakitsuka, M. Sugawara, Physics Review B 77 (2008) 195318.
[13] T. Warming, E. Siebert, A. Schliwa, E. Stock, R. Zimmermann, D. Bimberg, Physics Review B 79 (2009) 125316.
[14] C. Kindel, S. Kako, T. Kawano, H. Oishi, Y. Arakawa, G. Hönig, M. Winkelnkemper, A. Schliwa, A. Hoffmann, D. Bimberg, Physics Review B 81 (2010) 241309.
[15] A. Schliwa, M. Winkelnkemper, D. Bimberg, Physics Review B 76 (2007) 205324.
[16] S. Tomić, N. Vukmirović, Physics Review B 79 (2009) 245330.
[17] T. Nakaoka, T. Saito, J. Tatebayashi, Y. Arakawa, Physics Review B 70 (2004) 235337.
[18] T. Saito, H. Ebe, Y. Arakawa, T. Kakitsuka, M. Sugawara, Physics Review B 77 (2008) 195318.
[19] G. Bir, G. Pikus, Symmetry and Strain Induced Effects in Semiconductors, Wiley, 1974.
[20] L. Landau, E. Lifshitz, Theory of Elasticity, Pergamon Press, Oxford, 1970.
[21] F. Widmann, B. Daudin, G. Feuillet, Y. Samson, J.L. Rouvière, N. Pelekanos, Journal of Applied Physics 83 (1998) 7618.
[22] M. Arlery, J.L. Rouvière, F. Widmann, B. Daudin, G. Feuillet, H. Mariette, Applied Physics Letters 74 (1999) 3287.
[23] O. Marquardt, D. Mourad, S. Schulz, T. Hickel, G. Czycholl, J. Neugebauer, Physics Review B 78 (2008) 235302.
[24] K.B. Hong, M.K. Kuo, Semiconductor Science and Technology 25 (2010) 065005.
[25] K.B. Hong, M.K. Kuo, Semiconductor Science and Technology 25 (2010) 115015.
[26] M. Tadic, F.M. Peeters, K.L. Janssens, M. Korkusinski, P. Hawrylak, Journal of Applied Physics 92 (2002) 5819.
[27] R.V.N. Melnik, Applied Mathematics and Computation 107 (2000) 27.
[28] R.V.N. Melnik, M.N. Moskalkov, Differential Equations 27 (7) (1991) 860.
[29] R.V.N. Melnik, K.N. Melnik, Applied Mathematical Modelling 24 (2000) 147.
[30] R.V.N. Melnik, K.N. Zotsenko, Applied Numerical Mathematics 48 (2004) 41.
[31] R.V.N. Melnik, R. Mahapatra, Computers & Structures 85 (2007) 698.
[32] X. Peng, P. Logan, Applied Physics Letters 96 (2010) 143119.
[33] I.M. Lifshits, L.M. Rosentsveig, Zh. Eks. Teor. Fiz. Soviet Physics Journal of Experimental and Theoretical Physics (JETP) 17 (9) (1947) 783.
[34] F.C. Buroni, A. Sáez, Proceedings of the Royal Society A 466 (2010) 515.
[35] J. Nye, Physical Properties of Crystals, Clarendon Press, Oxford, 1957.
[36] A.H. Meitzler, IEEE Standard on Piezoelectricity, IEEE Press (1987) 1–54.
[37] I. Vurgaftman, J.R. Meyer, Journal of Applied Physics 94 (2003) 3675.
[38] S.M. Komirenko, K.W. Kim, M.A. Stroscio, M. Dutta, Physics Review B 59 (1999) 5013.
[39] E.O. Kane, Journal of Physics and Chemistry of Solids 1 (1957) 249.
[40] P.-O. Löwdin, The Journal of Chemical Physics 19 (1951) 1396.
[41] P. Rinke, M. Winkelnkemper, A. Qteish, D. Bimberg, J. Neugebauer, M. Scheffler, Physics Review B 77 (2008) 075202.
[42] J.Y. Fu, M.W. Wu, Journal of Applied Physics 104 (2008) 093712.
[43] M. Winkelnkemper, A. Schliwa, D. Bimberg, Physics Review B 74 (2006) 155322.
[44] S.L. Chuang, C.S. Chang, Physics Review B 54 (1996) 2491.